1995 NASA/ASEE SUMMER FACULTY FELLOWSHIP PROGRAM
JOHN F. KENNEDY SPACE CENTER
UNIVERSITY OF CENTRAL FLORIDA

SCHLIEREN OPTICS FOR LEAK DETECTION

Dr. Robert E. Peale, Assistant Professor
Mr. Patrick L. Summers, Student
Physics Department
University of Central Florida
Orlando, Florida

Mr. Alranzo B. Ruffin, Student
Physics Department
University of Michigan
Ann Arbor, Michigan

KSC Colleague - Carolyn McCrary
Instrumentation and Hazardous Gas Monitoring

Contract Number NASA-NGT-60002
Supplement 19

August 10, 1995

ABSTRACT

The purpose of this research was to develop an optical method of leak detection. Various modifications of schlieren optics were explored with initial emphasis on leak detection of the plumbing within the orbital maneuvering system of the space shuttle (OMS pod). The schlieren scheme envisioned for OMS pod leak detection was that of a high contrast pattern on flexible reflecting material imaged onto a negative of the same pattern. We find that the OMS pod geometry constrains the characteristic length scale of the pattern to the order of 0.001 inch. Our experiments suggest that optical modulation transfer efficiency will be very low for such patterns, which will limit the sensitivity of the technique.

Optical elements which allow a negative of the scene to be reversibly recorded using light from the scene itself were explored for their potential in adaptive single-ended schlieren systems. Elements studied include photochromic glass, bacteriorhodopsin, and a transmissive liquid crystal display. The dynamics of writing and reading patterns were studied using intensity profiles from recorded images. Schlieren detection of index gradients in air was demonstrated.

SUMMARY

The research described here consisted of a series of simple experiments designed to determine the suitability of a variety of optical schemes for detecting leaks. All schemes are variations of the classic schlieren method, which enhances imaging of index gradients by blocking undeflected rays. This work can be divided into two parts.

The first is an investigation of so-called zebra schlieren with emphasis on leak detection in the orbital maneuvering system of the space shuttle (OMS pod). A high contrast pattern (e.g. zebra stripes on reflecting cloth) is imaged onto a negative of this pattern (e.g. a Ronchi ruling), so that only rays deflected by a disturbance can pass the image plane. We find that the sensitivity of this technique is highest close to the imaging optics and far from the zebra stripes, precisely opposite of what is desired for the OMS pod situation. Simple considerations of geometrical optics explain this observation. An estimate of the maximum deviation expected from, for example, a He leak permits an estimate of the necessary length scale for the zebra pattern. This scale is so fine that loss of contrast in the image is expected from considerations of modulation transfer efficiency and a simple experiment. Hence, it appears that fundamental physical limitations will prevent this method of optical leak detection from finding use in OMS pod processing.

The second stage of the research concentrated on potential schemes for single ended schlieren. Here, the illuminated high contrast pattern is eliminated and a brightly lit outdoor scene is substituted, but the basic idea is the same. The negative of the distant scene must exist in the image plane, and the significant new idea here is to write this negative using reversible media. Media studied were photochromic glass, bacteriorhodopsin, and a transmissive liquid crystal display. Procedures for measuring the modulation of the written pattern and the dynamics of writing and reading the pattern were developed. Schlieren imaging was demonstrated in the laboratory, suggesting that single ended schlieren is nearly ready for field tests. Prototype designs based on each of the reversible media are suggested. A successful single ended schlieren system will have far reaching applications beyond and including the needs at Kennedy Space Center.

TABLE OF CONTENTS

LIST OF ILLUSTRATIONS

I
INTRODUCTION

Gaseous leak detection is an important problem at Kennedy Space Center, as it is in any large scale industrial activity. The leaks can be classified roughly into two types according to the geometry of the situation. The first type are those which occur in an enclosed and cluttered environment such as the internal plumbing associated with rocket engines. The second are those which occur in large open spaces, such as overland transfer lines, where remote sensing techniques are conceivable and desirable.

In this work, optical methods were explored for the imaging of leaks in both types of situations. The methods are variations of the classic schlieren optics[1]. Experiments described here begin with standard laboratory schlieren and work toward systems with industrial potential. Familiarity with principles and operating conditions at each step were sought and results were documented.

Many variations of schlieren optics have been developed during its long history[1]. By "standard" schlieren we mean all well established and documented variations. None of these is particularly useful for leak detection in industrial settings such as KSC, where the configuration of gas plumbing is determined by considerations other than convenience for schlieren. Specifically, in cramped and cluttered situations such as the internal plumbing of rocket engines the optics of a standard schlieren head cannot be placed around the test region. At the other extreme, for the situation of overland transfer lines, a standard schlieren head would need dimensions on the order of 100 m to simultaneously monitor the entire region of interest. In some situations, setting up of a schlieren head might be prohibited by safety concerns. Hence, a goal is remote schlieren having optics only near the operator.

II
STANDARD SCHLIEREN

Only one of the many classic schlieren variations will be described. Figure 2-1 presents a schematic of the optical set up. Two optical systems are superimposed. The first is the illumination and imaging system for the Ronchi ruling. This system is composed of a diffuse illuminator, a telescope mirror, and a Ronchi ruling (black stripes on glass with a 50% duty cycle). The diffuse illuminator (5 V lamp below 1/16 inch teflon) uniformly illuminates the lower half of the Ronchi ruling as shown. The Ronchi ruling is placed at the mirror's center of curvature (twice the focal length) and symmetrically about the optical axis so that the illuminated half is below the axis. An inverted image of the illuminated part is formed above the axis with unity magnification and is superimposed on the unilluminated part. By moving the Ronchi ruling perpendicular to the optical axis (vertically in Fig. 2-1) the dark parts of the image can be made to line up with the open stripes of the physical ruling. When this occurs, no light will pass the ruling.

To set this system up, look through the upper half of the ruling with your eye located where the camera is in Fig. 1. Then move the ruling together with your head in a plane perpendicular to the optical axis until the illuminated part of the ruling is observed in the mirror. Now move the ruling and your head along the axis until the virtual image fills the mirror, which will then appear uniformly bright. At this point the ruling is nearly at the center of curvature, and stripes should be observed. Further motion along the axis will cause the stripes to increase in size and separation until a single bright or dark stripe fills the mirror.

The schlieren effect is easiest to explain when a dark field exists. Under these conditions, none of the light from the illuminated part of the ruling is getting past the upper part of the ruling. A phase object, such as an index of refraction irregularity in the gas between the mirror and the observer, can cause rays which pass through it to leave the group of rays which form the image of the lower ruling on the upper one. These deviated rays may fall on an open part of the upper ruling and get through. The second optical system operates with these rays.

The second optical system consists of an imaging apparatus, such as the camera shown in Fig. 2-1. The camera images the test region in front of the mirror onto a ccd. Larger index gradients within the test region permit more light to reach the camera so that the intensity distribution in the recorded image maps out the disturbance itself. In practice, imperfect cancellation of undisturbed

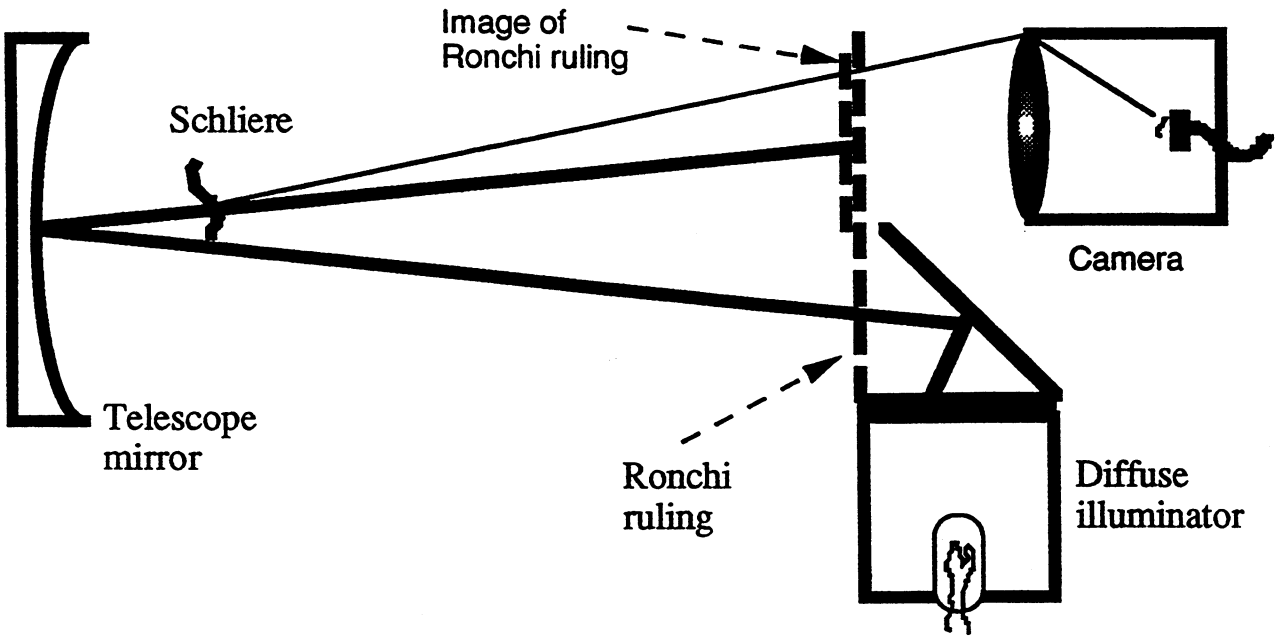

Figure 2-1. Standard schlieren optics.

rays by the first optical system permits an image of the disturbance to be formed with intensity changes of both signs and conveniently allows an image of reference objects to be simultaneously recorded.

Characteristic data collected with the standard schlieren apparatus of Figure 2-1 are presented in Figure 2-2. The data were recorded using an Elmo ccd television camera and the Macintosh based NuVision image processing system by Perceptics. In Fig. 2-2 the disturbance is caused by a squirt from canned air of the type used to dust electronic components. The gas is 1,1,1,2-tetrafluoroethane and has a refractive index significantly different from air. Intensity changes of both signs map out an image of the turbulent flow of gas from the nozzle, located just above and in front of the telescope mirror. None of the disturbance recorded here is visible to the naked eye. With this system, heat waves from warm body parts and even air conditioning currents are easily observed. This standard schlieren system is unsuited for leak detection in industrial settings like KSC because the telescope mirror is too bulky to use behind plumbing internal to rocket engines and too small to encompass the large areas traversed by overland transfer lines.

Figure 2-2. Test results of standard schlieren. Canned air is sprayed from the top and turbulence from the expanding jet is observed. Bright bands at the mirror edges are a result of spherical aberration.

III
ZEBRA SCHLIEREN

The following modified schlieren method is intended to eliminate the difficulty caused by the bulkiness of the mirror in situations with limited space, such as the interior plumbing of rocket engines. The name "zebra" comes from the striped pattern which is substituted for the mirror in Figure 2-1. Figure 3-1 presents a schematic of the zebra schlieren apparatus. Stripes made from black construction paper are placed in front of reflecting cloth (3M Corp.). The cloth is illuminated with a projector at close to normal incidence. The imaging optics are also placed close to this axis to take advantage of the strong return of the reflected beam in this direction. A projector is used instead of the diffuse illuminator because the return from the cloth is much less than from the telescope mirror. The zoom lens superimposes an image of the stripes on the Ronchi ruling, and the subsequent theory of operation is similar to that of the standard schlieren. The procedure used to set it up is different however.

Initial alignment is done with the Ronchi ruling removed from the set up. First the focus of the zoom lens is set to infinity to move the focal plane for the nearby zebra stripes back as far as possible. This allows more room for placement of the Ronchi ruling. A simple lens of short focal length is adjusted so that the image formed by the zoom lens is separated from the simple lens by its focal length. Rays leaving this lens are then parallel. The camera is focused at infinity to form an image from these parallel rays. This arrangement allows translation of the camera along the optical axis without losing focus. In particular, the camera can be placed directly behind the simple lens so that the object of interest fills its field of view. Everything is set up correctly when a sharp image of the zebra stripes appears on the TV monitor.

The front of the zoom lens is now blocked and the Ronchi ruling is inserted at the location of the stripe image behind the zoom. A sharp image of the Ronchi ruling should appear on the TV screen. The zoom is unblocked so that the image of the stripes is superimposed on the Ronchi ruling. Moire fringes will be seen in the TV monitor if the image of the stripes has a different scale than the Ronchi ruling. The Ronchi ruling is the correct distance from the zoom when this Moire pattern has its maximum contrast. The Ronchi ruling has the correct orientation when the Moire pattern is parallel with the direction of the stripes. By adjusting the zoom the scale of the image of the stripes can be matched with the scale of the Ronchi ruling. As this condition is approached, the separation of the Moire bands and their width increases until a single dark or light band fills the view. The focus of the zoom may have to be readjusted by monitoring the contrast of the Moire band since changing the zoom causes a change in the position of the stripe image. The Ronchi ruling can now be translated perpendicular to the optical axis to get the appropriate level of extinction. This translation is sensitive and best done with a micrometer stage.

All of the above steps are performed with the simple lens placed so that the camera images the stripes and Ronchi ruling simultaneously. If a disturbance is placed close to the zebra stripes, it will also be in focus with respect to the camera, but will nevertheless be invisible. We find that zebra schlieren is insensitive to disturbances close to the stripes. Placing the disturbance close to the entrance aperture of the zoom gives the best sensitivity, but the simple lens must be moved back so that the image of the disturbance formed by the zoom is at the simple lens's focal point.

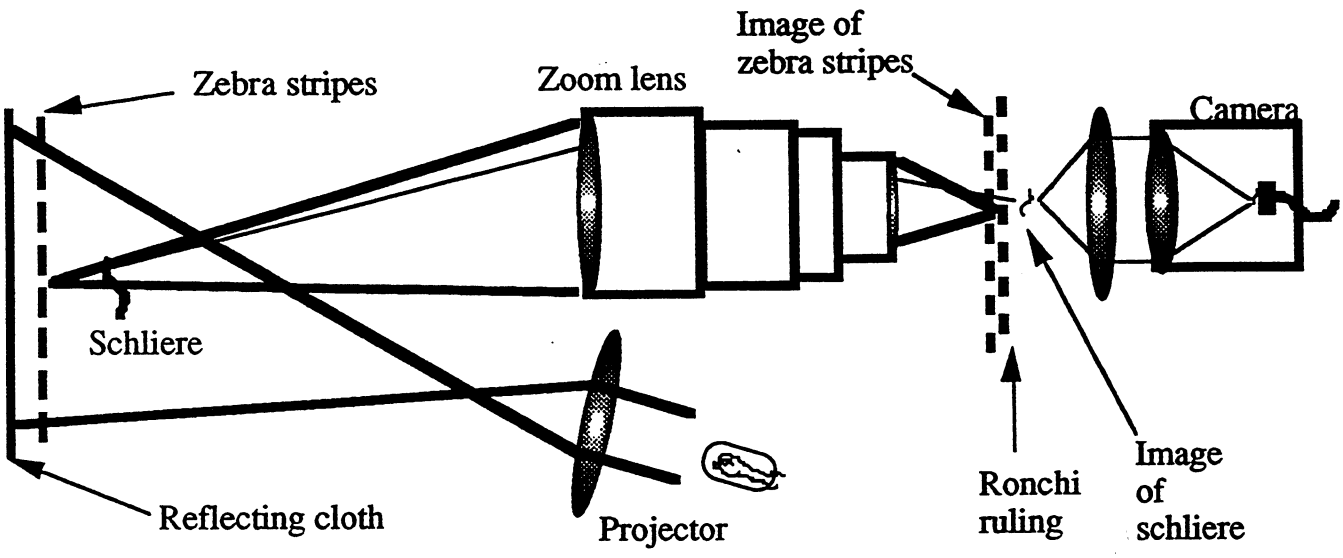

Figure 3-1. Zebra schlieren optics. An illuminated high contrast stripe pattern is precisely imaged onto its negative (Ronchi ruling). Ordinary rays are blocked and deviated rays form an image of the disturbance farther back. This image is viewed with the ccd camera.

Figure 3-2 presents data taken with the zebra schlieren set up. A jet from the inert gas duster is imaged just in front of the zoom. The zebra stripes and Ronchi ruling are out of focus and therefore invisible. The zebra schlieren method studied here is much less sensitive than the standard schlieren, where the turbulent plume of gas can be observed far down stream, as shown in Fig. 1-2. The stream recorded in Fig. 3-2 can also be seen with the naked eye (shadowgraph) though Fig. 3-2 records a significant enhancement. Heat waves from warm body parts were not observed. The actual set up can be significantly improved by fitting the critical optical elements

Figure 3-2. Test results of zebra schlieren. The canned air nozzle is placed just in front of the zoom lens. The distant illuminated stripe pattern is out of focus.

with micrometer stages, but the region of sensitivity will still be far from the stripes as will be shown next.

Figure 3-3 gives the pertinent geometrical parameters for zebra schlieren. For the schlieren effect, the disturbance must be large enough that deflected rays from a bright stripe appear to the

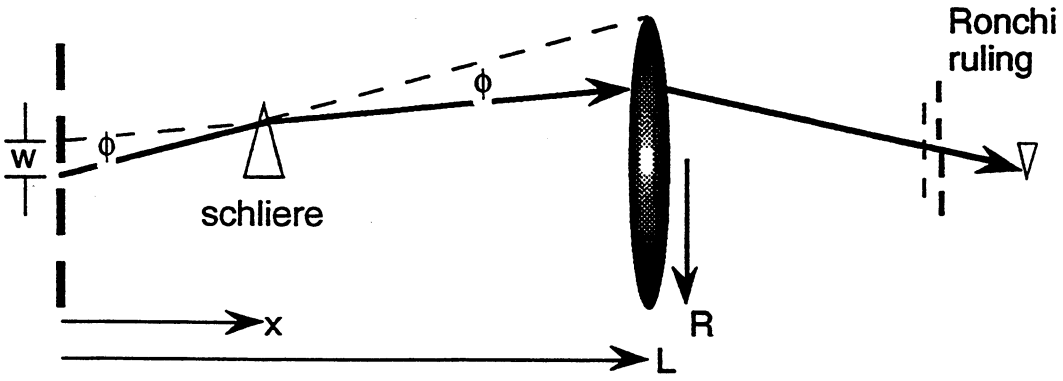

Figure 3-3. Geometrical considerations for zebra schlieren. An image of the stripe pattern is formed in registration with the Ronchi ruling. Rays which pass to form an image of the disturbance appear to subsequent optics to have originated in a dark stripe.

camera to have originated from a neighboring dark stripe. Also the deflection must be sufficiently small that deflected rays are collected by the zoom lens. Both conditions imply a minimum distance x for the disturbance from the stripes for a given deflection ϕ. These are $x \geq w/\phi$ and $x \geq L - R/\phi$.

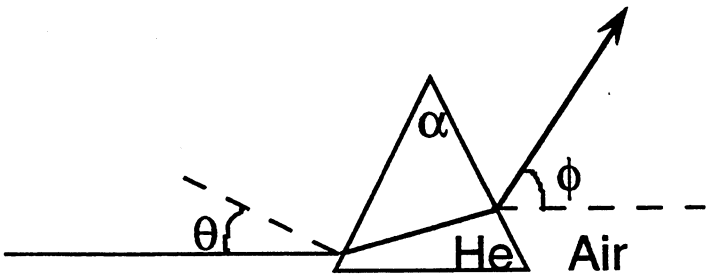

$$\phi = \theta - \alpha + \sin^{-1}[\sin\alpha\,(n^2 - \sin^2\theta)^{1/2} - \sin\theta\,\cos\alpha]$$

$$n = n(He) / n(air)$$

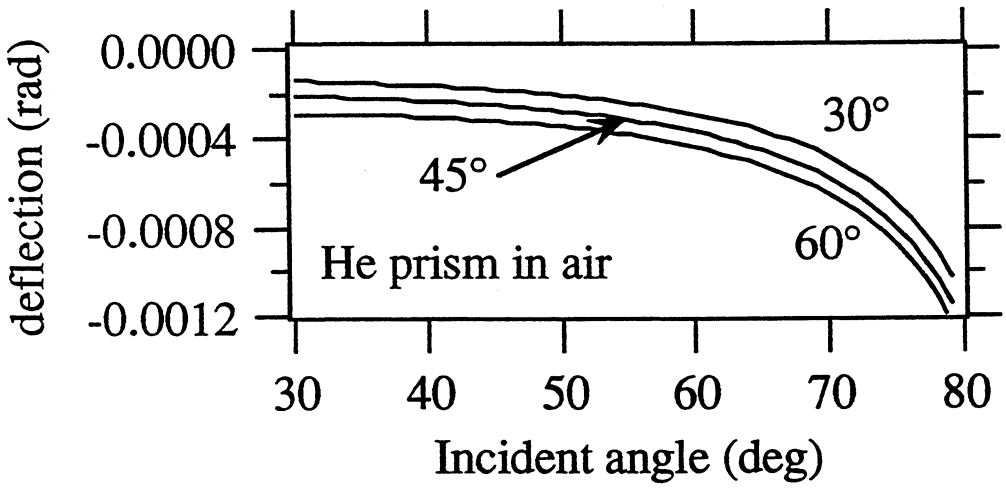

Figure 3-4. Estimate of expected deviation from He leak. A He leak is modeled as a isosceles prism with angle α. The incident angle is θ, and the deflection is ϕ. The formula gives ϕ in terms of α and θ, and the plot presents results for the range of α and θ that the majority of rays are likely to encounter. The maximum deviation is on the order of 1 mrad.

To determine which condition on x is more important for the OMS pod application, where x and L are fixed by external constraints, we must estimate the expected deviation ϕ. Figure 3-4 presents an estimate of the deviation expected from a bubble of He gas in air. The shape of a prism is assumed for simplicity. The formula for ray deviation by a prism is presented and can be found in any elementary optics text[2]. The index of refraction of air is 1.000293. That of He is 1.000036. The sign of the deflection is opposite that of a glass prism in air. The plot in Fig. 3-4 gives the deviation angle in radians for a range of incident angles and prism angles expected to be encountered by the majority of rays assuming a random orientation of prisms in the beam. The maximum deviation is 1 mrad at large angles of incidence. Relatively few rays are expected to have larger angles of incidence that those considered in Fig. 3-4 and their contribution to the effect will therefore be small. This treatment ignores multiple deflections by multiple He bubbles.

The geometry of the plumbing within the OMS pod is such that the stripes can be no farther than about 1 inch behind the plumbing being tested. For deviations of 1 mrad and optics on the order of 1 inch radius, the condition of acceptance of rays by the optics is unimportant for distances $L < 80$ ft. Hence the condition on stripe width prevails under circumstances likely to be encountered. With $x = 1$ inch and $\phi = 1$ mrad, we obtain stripe widths $w \leq 0.001$ inch. This is a very small dimension to work with. Assuming a high contrast pattern of such scale can be produced, the physical limitation is likely to be in imaging this pattern on a Ronchi ruling, which would have to be even smaller. Aside from the difficulty of alignment with the inevitable primary (Seidel) aberrations, there is the loss of contrast caused by diffraction. Rather than consider theoretically the decrease in modulation transfer function at high spatial frequencies caused by diffraction from finite aperture optics[2], we present the following simple experimental demonstration of the problem.

Figure 3-5 presents the experimental demonstration of loss of modulation transfer efficiency at high spatial frequency. Images of Ronchi rulings of successively higher line density are projected on a screen with magnification 3.5. As the data show, the contrast between light and dark fringes decreases until at 100 lines per inch, the lines disappear. (The complete disappearance at highest line density is partly due to additional loss of contrast in recording the image. Some modulation is still observed visually.) This demonstrates the fundamental physical difficulty in imaging fine patterns, and is in addition to aberrations (also observed in Fig 3-5) which cause loss of focus at even small distances from the optical axis. Hence, use of zebra schlieren for leak detection in confined geometries such as the internal plumbing of rocket engines appears unpromising.

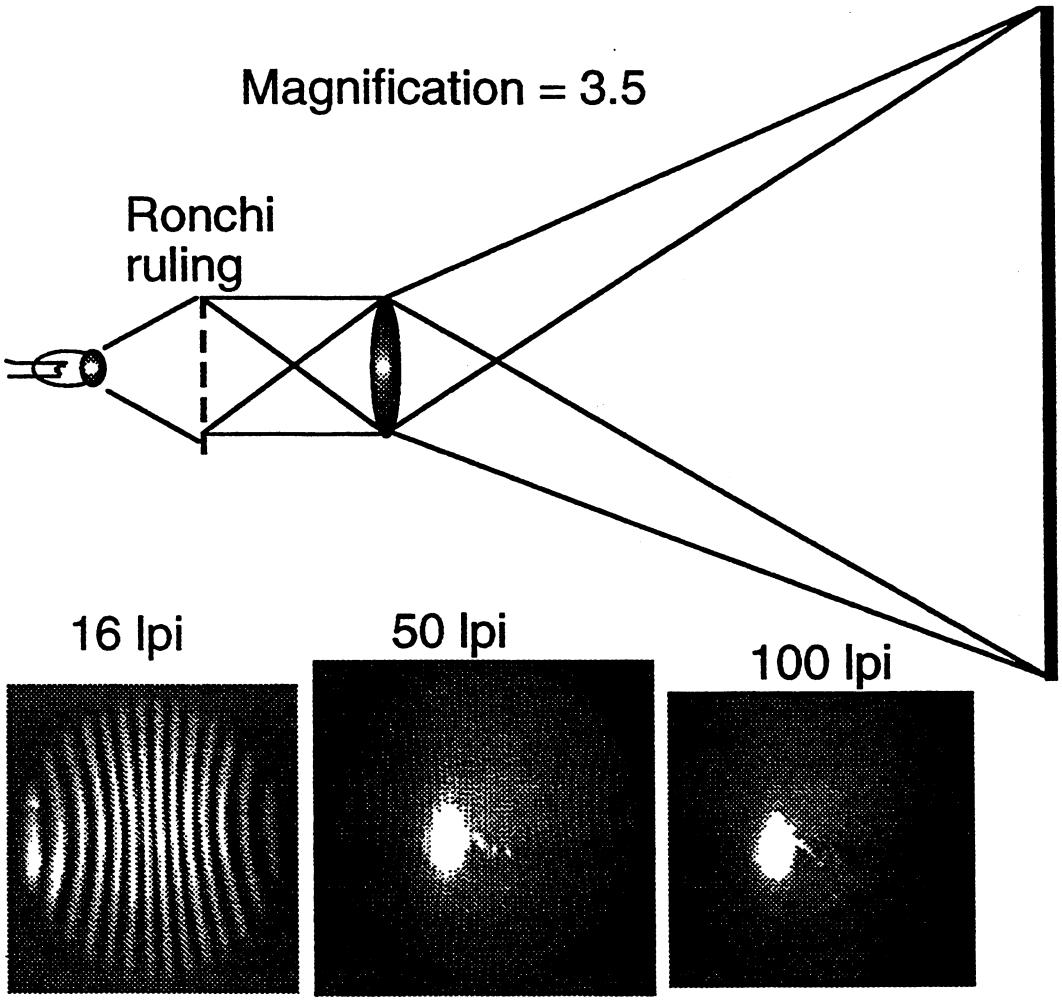

Figure 3-5. Projected Ronchi rulings. This plot demonstrates the well known loss of modulation transfer efficiency with increased spatial frequency. The data are digital photos of the projection screen for Ronchi rulings of different line densities.

IV
SINGLE-ENDED SCHLIEREN

We turn our attention now to the problem of leak detection over large areas, such as encountered with cross country transfer lines. As already said, standard schlieren is limited by the smallness of the available telescope mirrors to dimensions on the order of meters. Simultaneous monitoring of areas on the order of 100 m is desired.

As shown in the previous section, zebra schlieren is most sensitive far from the zebra stripe pattern. If the test region is to be remote from the imaging optics, then the zebra stripe pattern needs to be even further remote. The total area of the zebra pattern needs to be large so that it subtends a significant portion of the imaging system's field of view. This area requirement leads to significant practical difficulties. A new idea is needed.

A potential remedy is to eliminate the reflecting optics (mirror or stripes on cloth) altogether and to use instead a high contrast scene composed of natural elements such as clouds, trees, distant industrial structures, etc. This single ended schlieren scheme is presented in Figure 4-1. The basic principle of operation is identical to that of zebra schlieren. The significant difference is that the Ronchi ruling is replaced by a negative of the distant scene. Photographic negatives are impractical because of the required chemical processing. The ideal situation would be a material which could record the negative while in place within the schlieren system, thus guaranteeing perfect registration, and which could be easily erased to record new scenes.

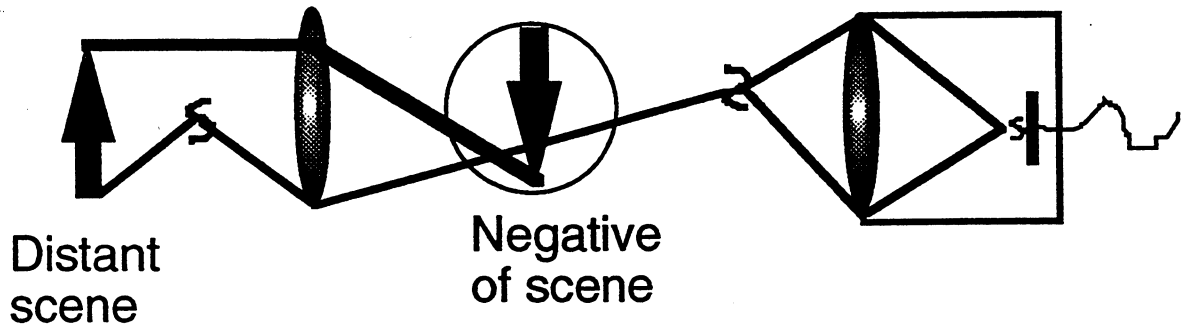

Figure 4-1. Single ended schlieren. The zebra stripes and Ronchi ruling of zebra schlieren have been replaced by a distant outdoor scene and its negative, respectively. In adaptive schlieren the negative is written on an erasable medium.

Three types of material were studied which have the ability to reversibly record the negative of a scene. The first is photochromic glass (Corning photogray) in which a photophysical transformation in microcrystals imbedded in a glass matrix is induced with UV light, causing the material to absorb visible light. The second is bacteriorhodopsin, in which exposure to light of one wavelength causes a reversible increase in absorption at a significantly different wavelength. The third is an electronic method in which a scene recorded with a CCD camera is sent to a transmissive liquid crystal display.

4.1 Photochromic glass

Figure 4-2 presents test results for the photochromic glass using a setup essentially identical to that in Fig. 4-1. The optical system looks into the muzzle of a UV curing gun. One picture is taken immediately after initial UV exposure. The other is after 10 minutes exposure where an obvious darkening is observed. These pictures where collected digitally with the NuVision system, which allows intensity profiles to be determined. The data plotted on the lower left of Fig. 4-2 are such profiles measured across the same part of each image. The contrast plotted on the right is the difference between the two profiles normalized by their sum. With this definition, the range of possible contrast values is 0 to 1. For the photochromic material a value of 0.15 is found. Even with contrast so much less than one, we have observed schlieren with this photochromic glass.

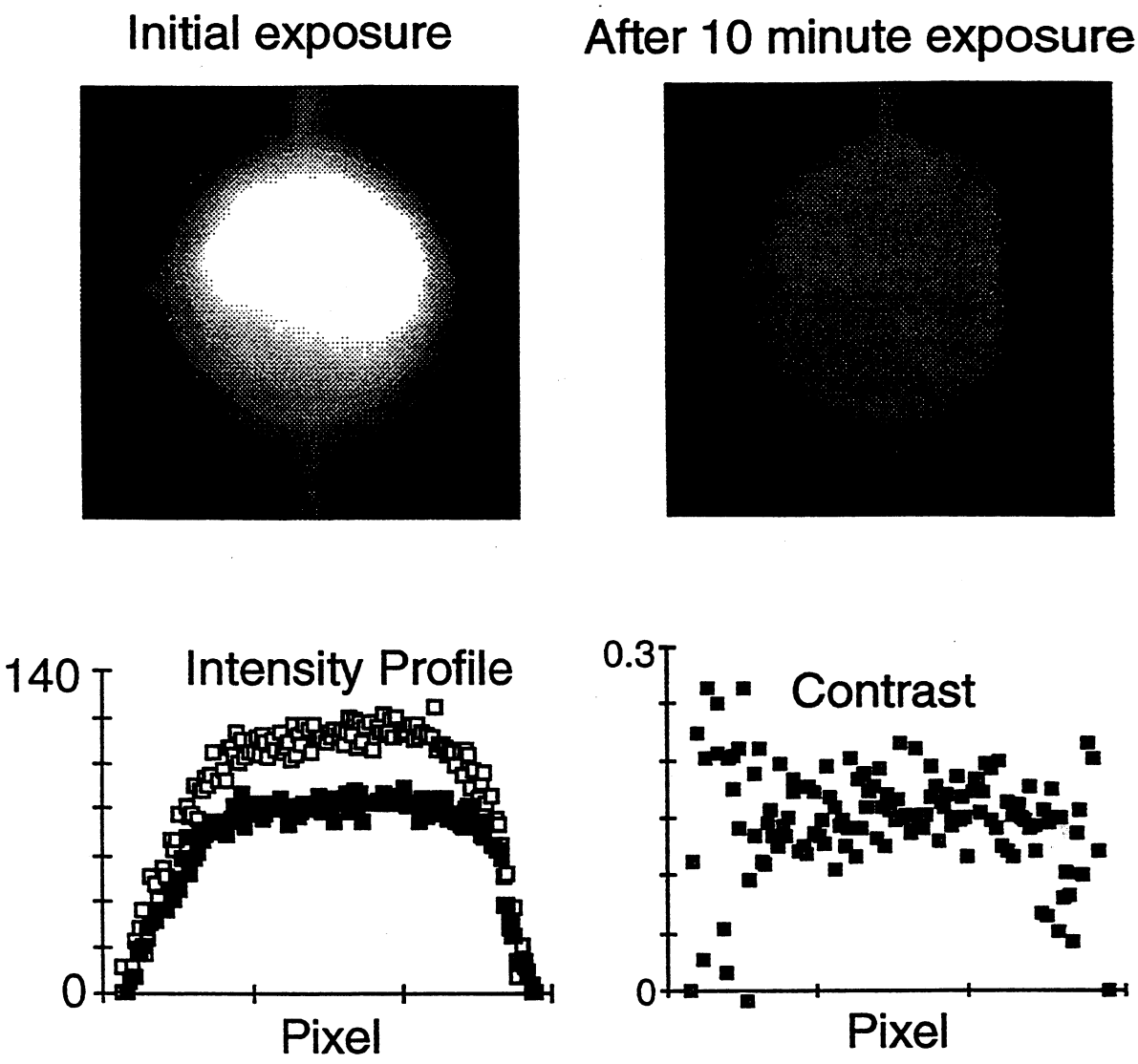

Figure 4-2. Contrast measurements with photochromic glass. The raw data are in the form of images of a UV curing lamp. Pictures are taken upon initial exposure and after 10 minutes. A darkening is evident. Intensity profiles are determined across the image and the contrast is calculated from them as their difference normalized by their sum.

4.2 Bacteriorhodopsin

Figure 4-3 presents a schematic of some of the spectral changes that can be induced in bacteriorhodopsin using monochromatic light[3]. In its ground "bR" state bacteriorhodopsin has an absorption band in the yellow which can be bleached by exposure to yellow light.

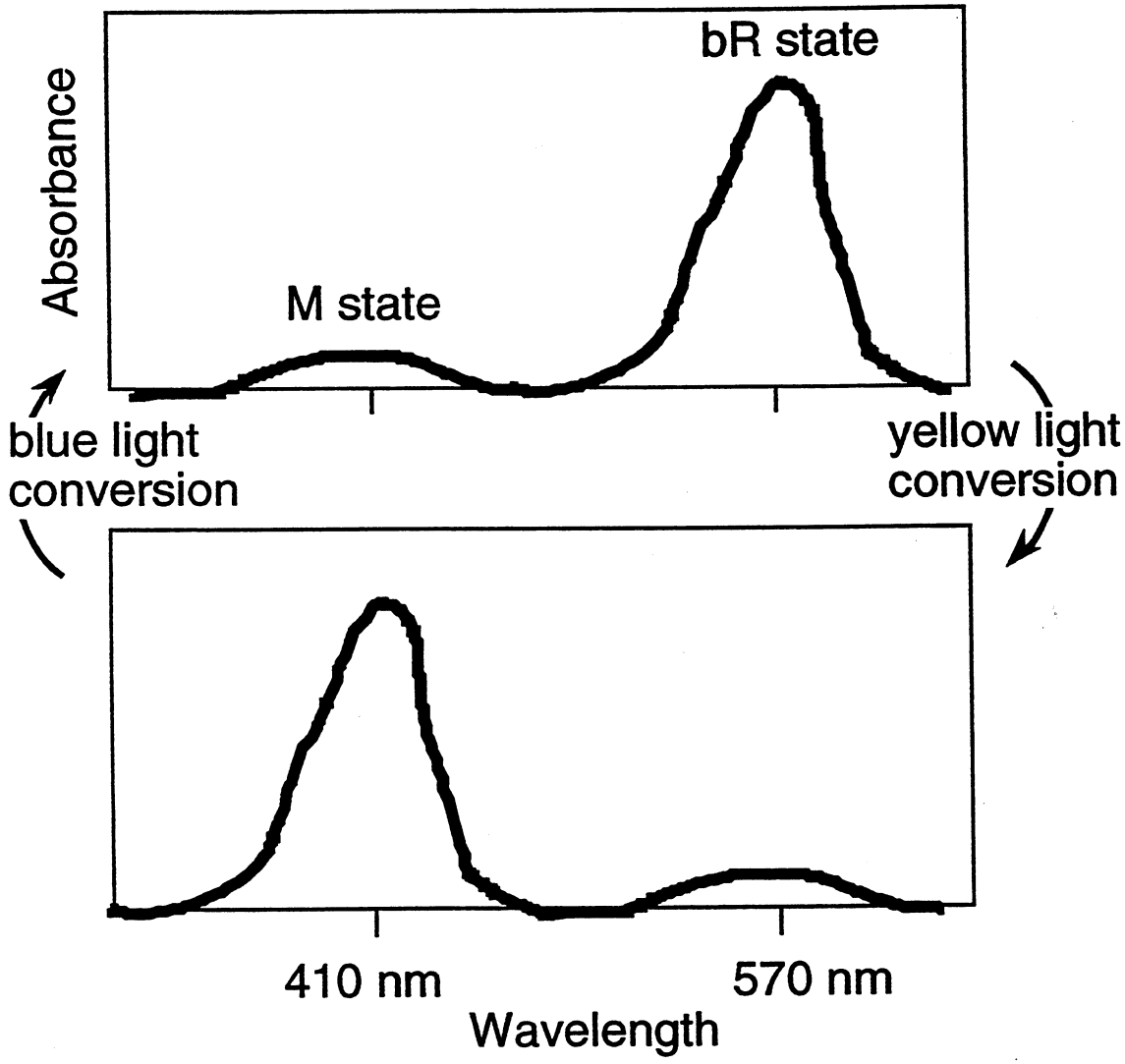

Figure 4-3. Schematic representation of bacteriorhodopsin photocycle.

The bleaching of the yellow band is accompanied by the appearance of an absorption band in the blue spectral region associated with the excited "M" state of the molecule. This phenomenon is the mechanism behind schlieren with bacteriorhodopsin: Exposure to an image in yellow light gives a negative of that image in blue light. One complication is that blue light induces a relaxation back to the bR state. The rate of this reverse reaction is controlled by the intensity of the blue light used. Part of our initial study of bacteriorhodopsin was to uncover the dynamics of the yellow writing and blue reading processes.

Figure 4-4 presents the results of the dynamics study using bacteriorhodopsin film sample number 107190A from Bend Research Inc.[4]. The set up was again like that in Fig. 4-1, except that the scene was a bright diffuse white light source. Colored filters were mounted in a cardboard holder on a slide in front of the film so that the exposure could be quickly alternated between yellow and blue. The filters used were Schott OG550, which passes light with wavelength longer than 550 nm, and Schott BG12, which is a band pass filter peaking at 400 nm. Neutral density filters were used to control the intensity of each color separately. The procedure was to collect an image using blue light, then expose the film to the same image in yellow light for a measured time, and finally quickly record the image in blue light again. Intensity profiles of the blue pictures before and after the yellow light exposure were obtained, and the contrast was calculated as before.

Figure 4-4a shows that the rate at which contrast is induced increases with the intensity of the yellow light used to burn the image. Moreover, the saturated contrast increases with the total intensity of yellow light used. This is because bacteriorhodopsin has a thermal relaxation pathway which proceeds at a constant rate for fixed temperature. The excited state population, and hence contrast, is determined by the balance in this relaxation rate and the excitation rate.

Figure 4-4b is a study of the erasing effect induced by blue light. The method here was to record the second blue image after varying delays. The contrast is seen to decay with blue-light exposure time at a rate which decreases as the blue light intensity is reduced.

Since the ultimate goal is single sided schlieren using ambient outdoor light, we performed writing and reading experiments using outdoor light as well. The door to the lab was opened and the optics aimed at the side of a building, which happened to be in shade. This light was sufficient to both write and read, as the data in Fig. 4-4 confirm. All the measurements in Fig. 4-4 are naturally very crude and preliminary. Timing was performed with wrist watches and the filters were moved in and out by hand. These measurements should be repeated with precisely timed electronic shutters or more elaborate time resolved spectroscopy. Nonetheless, our results describe the basic photodynamics of bacteriorhodopsin.

The maximum contrast obtained in our experiments with bacteriorhodopsin was 0.2. A standard schlieren apparatus similar to Fig. 2-1 was set up and schlieren was observed, as demonstrated in Fig. 4-5. Fig. 4-5a is a blue picture before yellow exposure. A hot soldering iron

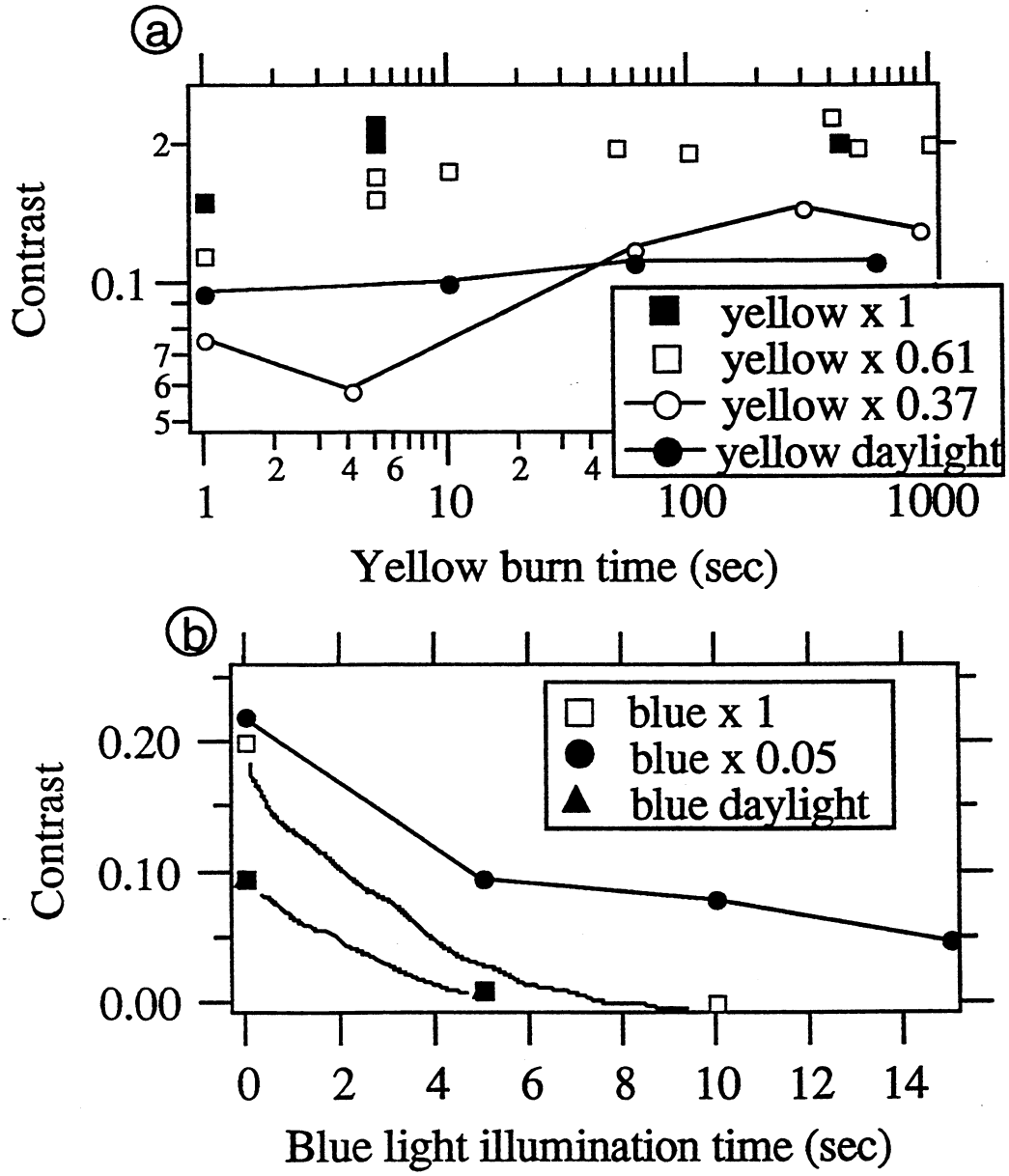

Figure 4-4. Bacteriorhodopsin write and read dynamics. Contrast is defined as the difference in intensity profiles normalized by the sum for images of a lamp taken in blue light before and after yellow light illumination. a) Maximum contrast is plotted against yellow light illumination time for different yellow light intensities. b) Contrast is plotted vs illumination time of the blue read light for different blue light intensities.

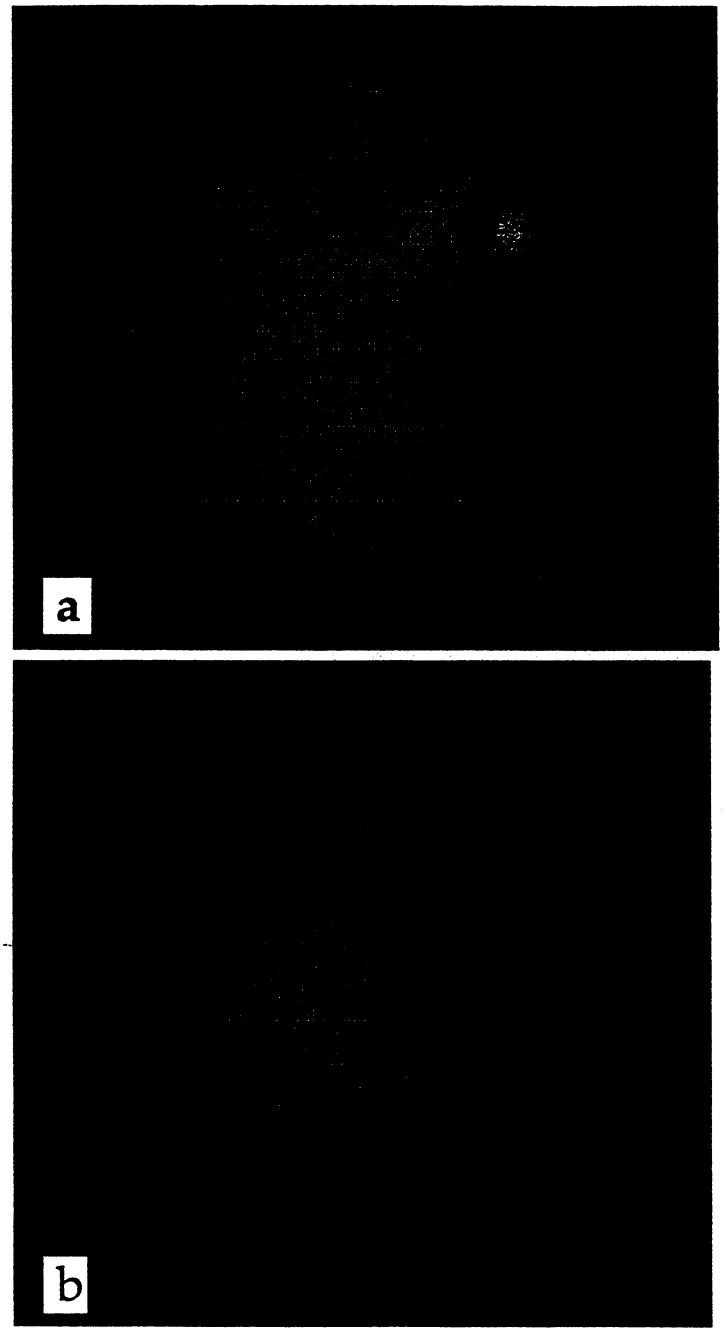

Figure 4-5. Bacteriorhodopsin schlieren test results. A soldering iron is in front of the telescope mirror at the bottom. a) Blue light image taken before yellow light illumination. b) Blue light image taken after yellow light illumination. Index disturbances are observed in the upper right.

is at the bottom edge of the telescope mirror. A 50 line per inch Ronchi ruling is imaged on the bacteriorhodopsin film by the mirror, but this image is out of focus with respect to the camera and is therefore not observed. Some scratches on the mirror surface are observed but otherwise the field is uniform and featureless. Figure 4-5b is a blue light picture taken after the Ronchi ruling has been written into the bacteriorhodopsin film with yellow light. An overall darkening is observed since now the bright stripes of blue are falling precisely on regions of the bacteriorhodopsin which have been made to absorb blue. In addition, the image appears mottled in the upper right quadrant as a result of index gradients induced by heat waves from the soldering iron.

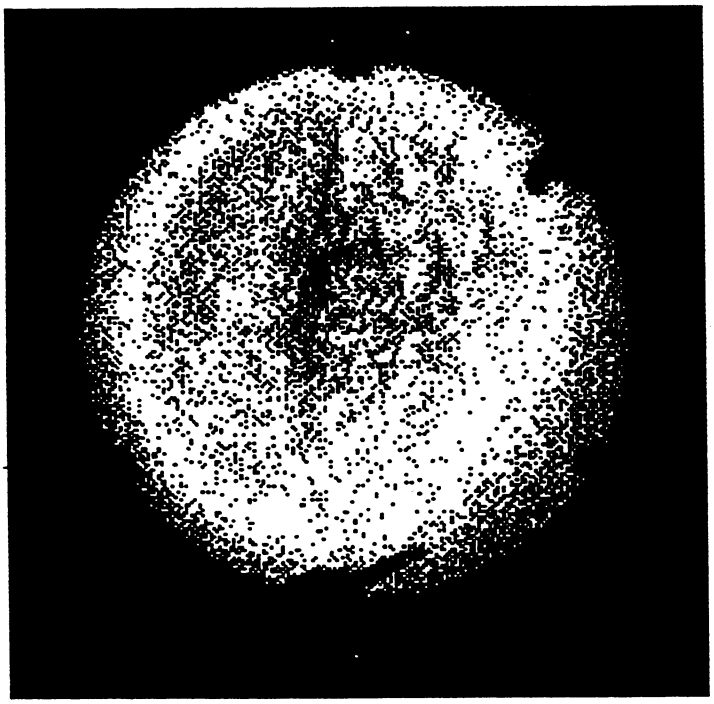

Fig. 4-6. Bacteriorhodopsin schlieren with image processing. Fig. 4-5a has been subtracted from Fig. 4.5b and a binary filter applied to the resulting histogram.

Figure 4-6 shows the same results as Fig 4-5 but with image processing applied. This picture has been included because it is expected to reproduce better than Fig. 4-5. In actuality, Fig. 4-5

contains more information, but this can only be appreciated fully when printed with photographic quality (on Tektronix Phaser IIsdx for example).

To verify that Figs. 4-5 and 4-6 represent a schlieren effect, a control was measured with the Rochi ruling removed. The same exposure steps were performed, except now the light on the film was uniform. The f-stop on the camera, which is behind the film, was stopped down by one to compensate for the two-fold intensity increase caused by removal of the 50% duty cycle Ronchi ruling. Hence, the pictures collected during the control appear to have the same level of brightness as those in Fig. 4-5. (The intensity of light falling on any part of the bacteriorhodopsin film is the same as that which fell in a bright region during the real experiment, but the average intensity entering the camera is doubled). The result of the control was that no effect such as seen in Figs. 4-5b and 4-6 was observed. Hence the Ronchi ruling is essential and Figs. 4-5 and 4-6 are a record of schlieren and not merely shadowgraph.

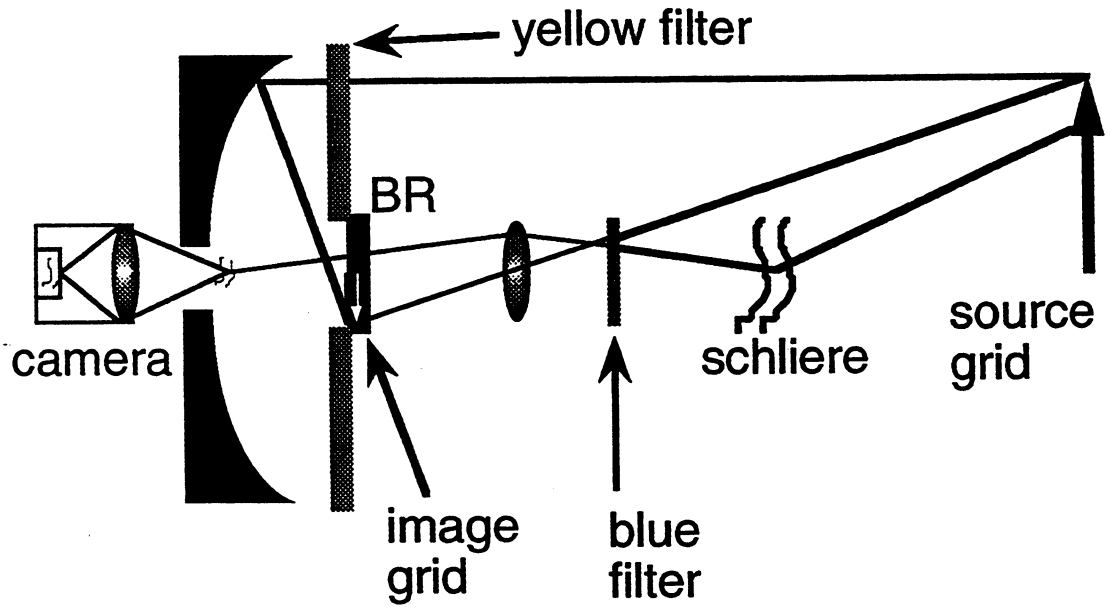

Figure 4-7. Scheme for steady state bacteriorhodopsin schlieren. A negative of the distant scene is continuously written in yellow light from the back side of the bacteriorhodopsin film. The scene is continuously observed in blue light through the front surface. The lens and mirror systems must have the same magnification, so it is convenient to use a zoom lens. Index changes of interest must be rapid compared with the characteristic write time of the bacteriorhodopsin film.

The transient nature of the bacteriorhodopsin write and read cycle is clearly undesirable in a practical device. Figure 4-7 presents a proposed alternative in which yellow write light and blue read light are always present. One disadvantage is that reading and writing is done with independent optical systems, so that automatic registration is lost. A zoom lens should be used to form the blue image. The relative intensities of yellow and blue light will have to be carefully adjusted with ND filters so that disturbances observed in blue are rapid compared with the change in the image stored in the film with yellow.

4.3 Liquid Crystal Display

Figure 4-8 presents the set up for a schlieren experiment using a transmissive LCD display. An illuminated stripe pattern on reflecting cloth is placed at the center of curvature of the mirror but displaced to the left of the optical axis. Initially the LCD is removed from the set up. The mirror forms an image of the stripe pattern with unity magnification to the right of the actual grid. The camera is focused on this image and displays it on the LCD, which acts as a TV monitor. The

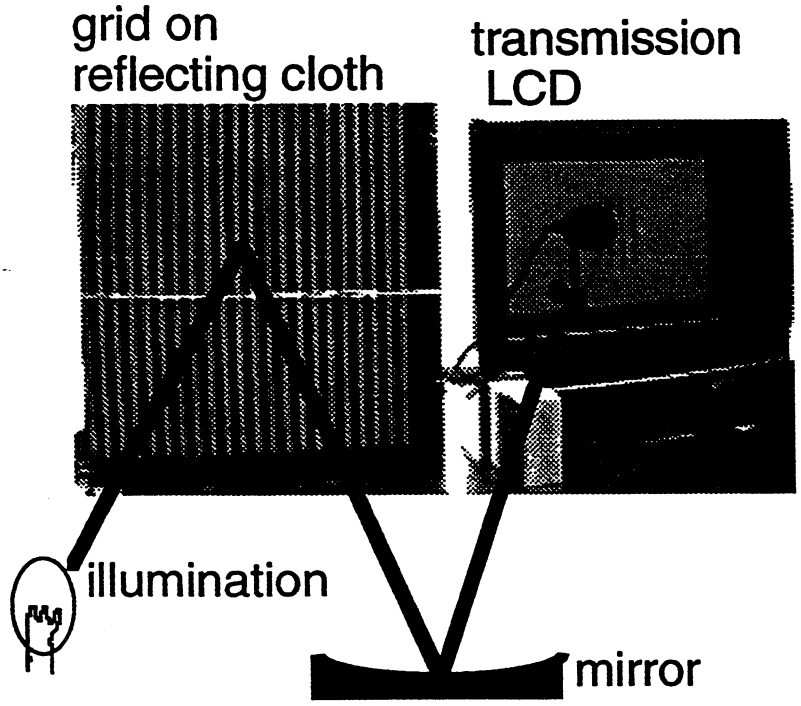

Figure 4-8. Set up for LCD schlieren experiment. The illuminated stripe pattern is imaged with the mirror onto a liquid crystal display, on which a freeze frame image of the pattern is displayed.

camera is moved back from the image plane until the stripes displayed on the LCD are the same width as those on the actual grid and its image. Now the display on the LCD is frozen using a frame grabber, and the LCD is returned to the set up. The camera is moved back close to the image plane so that the LCD picture fills the camera's field of view. The camera now looks through both the LCD and the grid image and is focused on the test region in front of the mirror. The LCD is translated perpendicular to the optical axis to put its displayed stripe pattern in registration with the image of the grid.

Figure 4-9 presents results obtained with the LCD schlieren apparatus just described. Heat waves are clearly visible from the soldering iron in front of the telescope mirror. It is important to realize that even with the LCD removed, a strong shadowgraph is observed which is enhanced by the non uniform illumination coming from the grid. However, sensitivity changes caused by LCD translation verify that a schlieren effect is present.

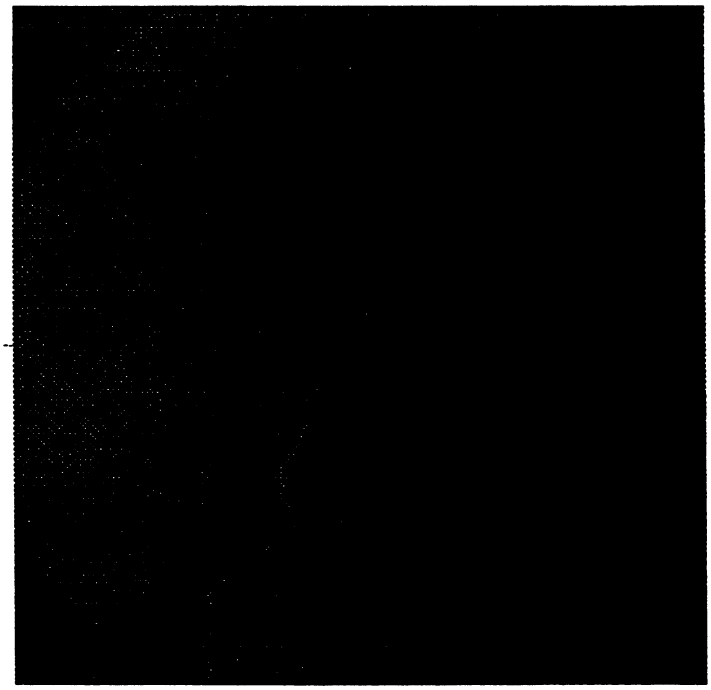

Figure 4-9. Results of LCD schlieren. Heat waves from a soldering iron are observed.

Limitations of the present LCD experiment are the coarseness of the pattern, the lack of sharp edges, limited contrast and resolution of the LCD. However, high-resolution transmissive LCDs do exist for heads-up display applications so that a compact arrangement like that of Fig. 4-1 can be envisioned with higher performance that realized so far.

V
CONCLUSIONS

Variations of schlieren optics have been explored with emphasis on leak detection. For leak detection within confined and cluttered situations (e.g. OMS pod), geometrical and optical considerations indicate a severely limited usefulness for the technique. On the other hand, single ended schlieren using adaptive optical elements such as photochromic glass, bacteriorhodopsin, and electrically controlled liquid crystal displays hold considerable promise as demonstrated by successful preliminary laboratory experiments.

Future work on single ended schlieren will explore other types of photochromic materials, bacteriorhodopsin schemes using continuous illumination and illumination modulated by electrically-switchable color filters [5], and small high-resolution LCDs. In addition, prototypes of actual systems will be developed and tested in field experiments.

REFERENCES

[1] For a collection of historical papers see Selected papers on schlieren optics, edited by Jurgen R. Meyer-Arendt, (SPIE milestone series; v. MS61, The International Society for Optical Engineering, Bellingham, WA, 1992)

[2]. Eugene Hecht and Alfred Zajac, Optics, Addison-Wesley, Reading, MA, 1979.

[3] D. Oesterhelt, C. Bräuchle, and N. Hampp, "Bacteriorhodopsin: a biological material for information processing", Quarterly Reviews of Biophysics **24**, 425-478 (1991).

[4]. Bend Research Inc., 64550 Research Road, Bend, Oregon 97701-8599.

[5] DisplayTech, Inc., 2200 Central Avenue, Boulder, CO 80301